J Musculoskelet Neuronal Interact 2022; 22(4):524-535

Journal of Musculoskeletal and Neuronal Interactions JMNI

Original Article

Effects of highly selective sensory/motor nerve injury on bone metabolism and bone remodeling in rats

Yadong Yang[1,2]*, Juan Zhou[3]*, Chen Liang[2], Qi Xiao[2], Yan Chen[4], Bo Yu[1]

[1]Department of Orthopedics, Zhujiang Hospital of Southern Medical University, Guangzhou, Guangdong, China;
[2]Department of Orthopedics, The First Affiliated Hospital of Gannan Medical University, Ganzhou, Jiangxi, China;
[3]School of Basic Medicine, Gannan Medical University, Ganzhou, Jiangxi, China;
[4]Ultrasound Medical Center, Zhujiang Hospital of Southern Medical University, Guangzhou, Guangdong, China
* contributed equally

Abstract

Objectives: This work aimed to investigate the mechanism of selective sensory/motor nerve injury in affecting bone metabolism and remodeling. **Methods**: The selective sensory/motor nerve injury rat model was constructed through posterior rhizotomy (PRG), anterior rhizotomy (ARG), or anterior combined with posterior rhizotomy (APRG) at the L_{4-6} sensory/motor nerves on the right side of rats. Sham-operated (SOG) rats served as control. At 8 weeks after surgery, the sciatic nerves, spinal cord segments L_5 and tibial tissues were collected for analysis. **Results**: the integrity of trabecular bone was damaged, the number of trabecular bone was decreased and the number of osteoclasts were increased in ARG group. ARG activated NF-κβ and PPAR-γ pathways, and inhibited Wnt/β-catenin pathway. ARG group exhibited high turnover bone metabolism. In PRG group, the trabecular bone morphology became thinner, and the number of osteoclasts was increased. NF-κβ pathway was activated and OPG/RANKL ratio was decreased in PRG group. The activated osteoclasts, reduced osteoblasts activity and lower turnover bone metabolism were observed in PRG group. Additionally, the bone metabolism in APRG group was similar to ARG group. **Conclusion**: The posterior rhizotomy and anterior rhizotomy induced the different degree of osteoporosis in rats, which may attribute to regulate Wnt/β-catenin, NF-κβ and PPAR-γ signalling pathways.

Keywords: Bone Metabolism, Bone Remodeling, Motor Nerve, Nerve Injury, Sensory Nerve

Introduction

Peripheral nerves significantly affect the progression of bone metabolism and bone remodeling[1,2]. The close anatomical relationship between bone and nerves also reflects the relationship among callus formation, bone remodeling, regeneration of injured nerve endings and new bone growth[3]. Furthermore, Hukkanen et al. have first confirmed that peripheral nerve injury negatively affects the mechanical integrity of the callus after fracture[4]. Therefore, studying the interaction between nerve injury and bone remodeling has potential therapeutic significance for fracture patients. In recent years, some scholars have observed the growth of sensory nerves in the callus of rats with tibial fractures after cutting the sciatic and femoral nerves[5], suggesting that the denervation model is not satisfactory. This model should first be improved for further investigating the effects of sensory/motor nerves on bone metabolism. Based on the improved model, the precise molecular mechanisms of sensory/motor nerve injury in regulating bone remodeling or bone metabolism can be studied more scientifically.

Wnt/β-catenin, nuclear factor-kappaB (NF-κβ) and peroxisome proliferator-activated receptor γ (PPARγ) signalling pathways are important for the regulation of

The authors have no conflict of interest.

Corresponding authors:
Yan Chen, Ultrasound Medical Center, Zhujiang Hospital of Southern Medical University, 253 Industrial Avenue, Haizhu District, Guangzhou, Guangdong, China 510285
E-mail: smu_chen@163.com
Bo Yu, Department of Orthopedics, Zhujiang Hospital, Southern Medical University, 253 Industrial Avenue, Haizhu District, Guangzhou, Guangdong, China 510285
Email: gzyubo@163.com

Edited by: G. Lyritis
Accepted 23 August 2022

bone remodeling and bone metabolism[6]. Wnt pathway can inhibit the differentiation of bone marrow mesenchymal stem cells (BMSCs) into adipocytes and chondrocytes, and promote the differentiation of osteoblasts and inhibit their apoptosis, thereby improving the mineralization ability of osteoblasts[7-9]. PPARγ has been found to be correlated with bone metabolism[10,11]. Specifically, PPARγ activation can down-regulate Runt-related transcription factor 2 (Runx2) and osteoblast-specific element 2 (OSE-2) expression, and thus suppresses osteocalcin expression and reduces osteogenesis[12-14]. Osteoprotegerin (OPG)/receptor activator of NF-κβ ligand (RANKL) signalling pathway is one of the upstream of NF-κβ, and OPG is the regulator of RANKL/RANK signalling pathway. The inhibition of RANK activation can be achieved by the binding of OPG to RANKL[15]. The regulatory relationship between peripheral nerve injury and these bone metabolism related signalling pathways has been reported. However, the effects of different nerve components on bone metabolism have not been reported. Hence, we selectively cut off the sensory/motor nerves of rats and studied the effects of the two different nerve injuries on these bone metabolism-related signalling pathway factors, and thus provided the basic theory for the prevention and treatment of fracture, osteoporosis and other related diseases.

Materials and methods

Animals

Adult female Sprague Dawley (SD) rats weighing 200-250 g were obtained from Animal Experiment Center of Research Center of Gannan Medical University (Gannan, China). Rats were housed at an ambient temperature of 20-25°C and a relative humidity of 50-60%. Rats were free access to water and food.

Animal model

A total of 40 SD rats were used in this study. Forty SD rats were randomly divided into 4 groups (n=10/group): sham operated group (SOG), posterior rhizotomy group (PRG), anterior rhizotomy group (ARG), anterior and posterior rhizotomy group (APRG). Rats were anesthetized by intraperitoneal injection of 10% chloral hydrate (250 mg/kg). Transection of the L_{4-6} sensory/motor nerves on the right side of rats was performed under a binocular operating microscope. Specifically, in SOG group, L_{4-6} nerve roots were exposed without posterior or anterior rhizotomy. In PRG group, the rats were subjected to posterior rhizotomy of L_{4-6} nerve roots, and the nerve roots were cut off by 2 mm. In ARG group, the rats were subjected to anterior rhizotomy of L_{4-6}, and the nerve roots were cut off by 2 mm. In APRG group, L_{4-6} sensory and motor nerve roots of rats were transected. At 8 weeks after surgery, rats were euthanized by cervical dislocation. The sciatic nerves, spinal cord segments L_5 and tibial tissues were collected from rats for further use.

Postoperative care

To prevent postoperative infection, the incision was washed with iodophor at the end of the operation. Then, 1.6 million units of penicillin was sprinkled into the incision. After the operation, the rats were kept in a single cage to prevent each other from biting the surgical site. The bedding of rats was changed every other day. The surgical site was cleaned and disinfected with an iodophor cotton swab every day. The surgical site was healed after a week.

Differences in animal behavior after unilateral dorsal and/or ventral root injury

(1) ARG group (ventral root injury): When the rats walked, the lower limbs on the side with nerve root injury cannot actively flexion and extend. There was no muscle contraction activity in the lower limbs of the severed nerve side, and the muscle atrophy was obvious observed. The lower limbs of the severed nerve side could not walk actively and showed a dragging gait. When a needle was used to stimulate the lower limbs of the severed nerve side, rats cried but the lower limbs could not move. (2) PRG group (dorsal root injury): the lower limbs on the side with nerve root injury could walk normally, but the lower limbs were swollen. Some rats developed foot ulcers, and the walking speed was slower than that of the SOG group. When a needle was used to stimulate the lower limbs of the severed nerve side, rats were silent but the lower limb could move. (3) APRG group (both ventral and dorsal root injury): the behaviors of the rats were similar to that of the ARG and PRG groups. Rats developed sensory nerve ulcers on the soles of their feet, and showing a distinct dragging gait. When a needle was used to stimulate the lower limb of the severed nerve side, the rat was silent and the lower limb could not move.

Osmic acid staining

The sciatic nerves of rats were fixed with 4% paraformaldehyde for 24 h. After that, the nerves were rinsed with running water and fixed with 1% osmic acid for 24 h. The nerves were dehydrated with gradient concentrations of ethanol, vitrified with dimethylbenzene, and embedded in paraffin. The paraffin-embedded samples were sliced into sections with 1 μm. Finally, the sections were observed under an optical microscope with image acquisition system, and the numbers of sensory nerve fibers, motor nerve fibers, sympathetic nerve fibers and total nerve fibers were counted utilizing Image Pro-plus software.

Sympathetic nerve fibers can be divided into myelinated nerves and unmyelinated nerves according to their location. The sympathetic nervous system consists of two populations of neurons, namely preganglionic sympathetic neurons and postganglionic sympathetic neurons that are anatomically organized in series and connected synaptically[16]. Among them, most of the preganglionic nerve fibers belong to myelinated nerves, and the postganglionic nerve fibers belong to unmyelinated nerves. The sympathetic nerves located in

the cervical spinal cord belong to postganglionic nerve fibers which are unmyelinated nerves. The sympathetic nerves of thoracolumbar spinal cord are located in the lateral horn. Their fibers originate from the corresponding spinal segment and terminate at the prevertebral ganglia, thus the fibers belong to preganglionic nerve fibers and myelinated nerves. After entering the ganglions to replace neurons, a longer postganglionic nerve fibers will be send out and delivered to the effector organs. Here, the sympathetic nerves in the sciatic nerve of the rat belongs to lumbar sympathetic nerves and are preganglionic nerve fibers, so they are myelinated nerve fibers. Hence, in this experiment, the number of sympathetic nerve fibers in the sciatic nerve was determined by counting myelinated nerve fibers.

Furthermore, healthy sciatic nerve fibers are myelinated nerve fibers, and the Osmic acid staining results of motor nerve fibers and sensory nerve fibers in histologically are same. The distribution of nerve fibers and the thickness of the myelin sheath are uniform in healthy sciatic nerve fibers, thus, the Osmic acid staining can only show the number of nerve fibers and the morphology of myelin sheath. In our experiments, the pathological changes in nerve fibers and myelin sheath after cutting the anterior or posterior roots of spinal cord, such as degeneration, collapse and absorption, were used to reversely infer whether the nerve fibers are sensory nerve fibers or motor nerve fibers. When the anterior roots of spinal cord were cut off, the myelin sheath of some nerve fibers in the sciatic nerve displayed degradation, collapses and absorption, and these nerve fibers are the motor nerve fiber. Meantime, the nerve fibers that had no changes in myelin sheath were sensory nerve fiber. When the posterior roots of spinal cord were cut off, the myelin sheath of some nerve fibers in the sciatic nerve displayed degradation, collapses and absorption, and these nerve fibers are sensory nerve fiber. Meantime, the nerve fibers that had no changes in myelin sheath were motor nerve fibers.

Immunohistochemical staining

Spinal cord tissues and bone tissues were fixed with 4% paraformaldehyde for 24 h. Bone tissues were decalcified with 10% ethylene diamine tetraacetic acid (EDTA) for 4 weeks. After that, spinal cord tissues and bone tissues were embedded in paraffin. After dewaxing and hydration, the paraffin sections (4 μm) of spinal cord tissues and bone tissues were incubated with sodium citrate buffer for antigen retrieval and blocked with bovine serum albumin. Subsequently, the sections were incubated with primary antibodies including NeuN (#GB13138-1; Servicebio, Wuhan, China), calcitonin gene related peptide (CGRP; #bs-0791R; Bioss, Beijing, China), RANKL (#GB11235; Servicebio), OPG (#GB11151; Servicebio), or osteocalcin (OCN; #bs-4917R; Bioss) overnight at 4°C, and then were incubated with the corresponding secondary antibody (Servicebio) at room temperature. Finally, the sections were observed under an optical microscope.

The nerves in the posterior horn of normal spinal cord are sensory nerves, and the nerves in anterior horn are motor nerves. The number of motor nerves is less than that of sensory nerves, but the volumes of motor nerves are larger than that of sensory nerves. Immunohistochemical staining for NeuN was utilized to mark neurons. The brown-yellow areas in the posterior horn of spinal cord represent sensory nerves with tiny brown-yellow granules. The brown-yellow areas in the anterior horn of spinal cord represent motor nerves with bulky brown-yellow granules. After removal of sensory nerves, the sensory nerves in the posterior horn of spinal cord were reduced or partially absent, while the motor neurons in the anterior horn of spinal cord were found to be reduced or partially absent after removal of motor nerves. To sum up, there are two ways to distinguish sensory nerves or motor nerves in the spinal cord. On one hand, the nerves in the posterior horn of normal spinal cord are sensory nerves, and the nerves in anterior horn are motor nerves. On the other hand, the brown-yellow granules in sensory nerves are small and much, and the granules in motor nerves are and large and little. The sections were photographed utilizing the Olympus DP50 image acquisition system, and then Image proplus image analysis software was used to count the number of motor nerves in anterior horns and the number of sensory nerves in posterior horns of the spinal cord.

Micro-CT

The tibia with 2 cm length was fixed with 4% paraformaldehyde. After fixation, the tibia was scanned utilizing a micro-CT (SkyScan 1172, Belgium). The scanning parameters were shown as follow: slice thickness 10 μm, voltage 80 kVp, resolution 10 μm, current 500 μA, and exposure time 2000 ms.

The distal end of the tibial growth plate and tibial tissues with 2 mm thick was selected as region of interest (ROI). The data were imported into the Inveon Research Workplace 2.2 software for three-dimensional reconstruction of the sample microstructure. The bone remodeling caused by peripheral nerve injury was mainly manifested in the cancellous bone of the metaphysis of the limbs. Therefore, the structural parameters of the cancellous bone were analyzed on the basis of three-dimensional reconstruction. The main parameters of ROI included trabecular bone thickness (Tb. Th, μm), bone volume fraction (BV/TV, %), trabecular bone number (Tb. N, 1/mm), trabecular bone pattern factor (Tb. Pf, 1/mm), trabecular bone separation (Tb. Sp, μm) and bone mineral density (BMD, mg/cm^3).

Histochemical analysis

The bone tissues were subjected with fixation, decalcification and embedding. Then, the longitudinal serial sections with 4 μm were obtained along the longitudinal axis of the tibia. Hematoxylin-eosin (HE) staining and Tartrate-resistant acid phosphatase (TRAP) staining were carried out to observe the pathological changes of bone tissues following the previous reported[17]. Finally, the sections were observed under an inverted phase contrast microscope.

Quantitative real-time PCR (qRT-PCR)

Tibial tissues were minced and ground into power in the presence of liquid nitrogen. The tissue power was treated with Trizol reagent to extract total RNA from bone tissues. RNA was reverse transcribed into cDNA applying the reverse transcription kit (MBI Fermentas, Ontario, Canada). Finally, qRT-PCR was performed to detect the relative expression of mRNA applying TB Green Premix Ex Taq (Takara, Dalian, China). The primers used in qRT-PCR were designed and provided by Sangon Biotech (Shanghai, China). The primer sequences (5'-3') were shown as follows:
Wnts1: F-GCCAACAGTAGTGGCCGATG;
R-CTGGGCTCTAGCACCAGCTGTA;
LRP5: F-AGTGCGTGGACCTGCGTTTAC;
R-AATCGCACTGCTGCTTGATGAG;
TRAF6: F-AGAGGAATCACTTGGCACGG,
R-TCTGCGTTTCCATTTTGGCG;
NF-κβ: F-CCCACGGATGTTCACAGACA;
R-CTGTCGGAGAAGTTGGGCAT;
β-catenin: F-ACCATCGAGAGGGCTTGTTG;
R-CGCACTGCCATTTTAGCTCC;
β-actin: F-AGATGTGGATCAGCAAGCAG;
R-GCGCAAGTTAGGTTTTGTCA.
β-actin was used as reference gene for normalization. The results were analyzed using $2^{-\Delta\Delta CT}$ method for quantification.

Statistical analysis

The data were expressed as mean ± standard deviation (SD). SPSS 25.0 (IBM, Armonk, NY, USA) was used for statistical analysis. Data were analyzed by normality test, Homogeneity of variance test and one-way analysis of variance. A significant difference was suggested if $P<0.05$.

Results

Construction of the rat model with selective sensory/motor nerve injury

We first constructed selective sensory/motor nerve injury rat model through posterior rhizotomy or anterior rhizotomy, and evaluated the nerve injury in rats. The results obtained from Osmic acid staining revealed that SOG group displayed the myelinated nerve fibers with uniform diameter and myelin sheath thickness. Compared with SOG group, the sensory nerve fibers in the PRG group were degenerated, while a small amount of motor nerve fibers increased and remained in the muscular branches. It may be due to the increased painless activity after sensory nerve loss in rats. In ARG group, the motor nerve fibers were degenerated, while the number of sensory nerve fibers had no change. In the APRG group, both the sensory and motor nerve fibers were degenerated. A small number of myelinated nerve fibers was observed in the muscular branches, which was considered as sympathetic nerve fibers (Figure 1A-B). Furthermore, we used NeuN to label neurons and examined the expression of NeuN in the spinal cord segments L_5 of rats by immunohistochemistry. Compared with SOG group, sensory neurons had no changes in the ARG group, while were significantly reduced in the PRG and APRG groups. There was no difference in motor neurons between SOG and PRG groups. The decreased motor neurons were observed in the ARG and APRG groups when contrasted to SOG group (Figure 2A-B). All these results confirmed the rat model with sensory/motor nerve fiber injury was successfully constructed.

Effects of selective sensory/motor nerve injury on trabecular bone structure of rats

We observed the structural changes of the tibial profile and cancellous bone in rats through micro-CT. Compared with SOG group, the integrity of trabecular bone in ARG group was damaged, the number was reduced and the bone separation was increased. The bones in the ARG group showed an insect bite-like reaction, and the marginal trabecular bone displayed compensatory thickening. In PRG group, trabecular bone became thinner gradually, and its number decreased slightly. However, there was no obvious cavity in trabecular bone, and the integrity of trabecular bone was not damaged. Trabecular bone was also significantly thinner in the APRG group, with reduced numbers and compromised integrity. Numerous large cavities were observed in the center of the cancellous bone in APRG group (Figure 3A). Subsequently, the bone quality parameters were analyzed. Compared with SOG group, the parameters BV/TV, BMD, Tb. N, and Tb. Th were significantly decreased in PRG, ARG and APRG groups. Increased Tb. Sp and Tb. Pf were observed in PRG, ARG and APRG groups, especially in APRG group (Figure 3B). These results jointly confirmed that different nerve injury components may cause different degrees of tibial osteoporosis in rats.

Effects of selective sensory/motor nerve injury on pathological changes of trabecular bone of rats

HE staining was carried out to measure the pathological changes of trabecular bone in rats. Compared with SOG group, the decreased number of trabecular bone was observed in PRG, ARG and APRG groups. In PRG group, the trabecular bone was thin, but the trabecular bone was intact. In ARG group, the integrity of trabecular bone was partially damaged with bone resorption voids. The trabecular bone in the APRG group showed uneven thickness, disordered arrangement, poor integrity, and obvious voids (Figure 4).

Effects of selective sensory/motor nerve injury on osteoclasts of rats

TRAP staining uncovered the changes of osteoclasts in the tibial tissue of rats. As shown in Figure 5A-B, the number of osteoclasts was obviously increased in PRG, ARG and ARPG groups with respect to SOG group, especially in ARPG groups. The osteoclasts in PRG, ARG and ARPG groups were large in size and had numerous nuclei. Collectively, the

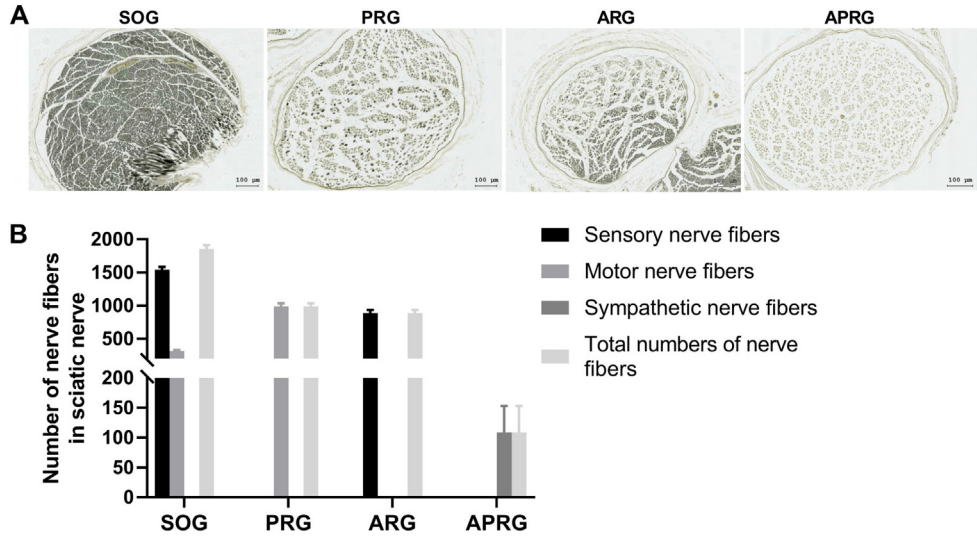

Figure 1. The myelinated nerve fibers in the sciatic nerves of selective sensory/motor nerve injury rats. Rats were subjected to posterior rhizotomy (PRG), anterior rhizotomy (ARG), or anterior combined with posterior rhizotomy (APRG). Sham-operated (SOG) rats served as control. (A-B) Osmic acid staining was carried out to examine the numbers of sensory nerve fibers, motor nerve fibers, sympathetic nerve fibers and total nerve fibers in the sciatic nerves of rats. Scale bar =100 μm.

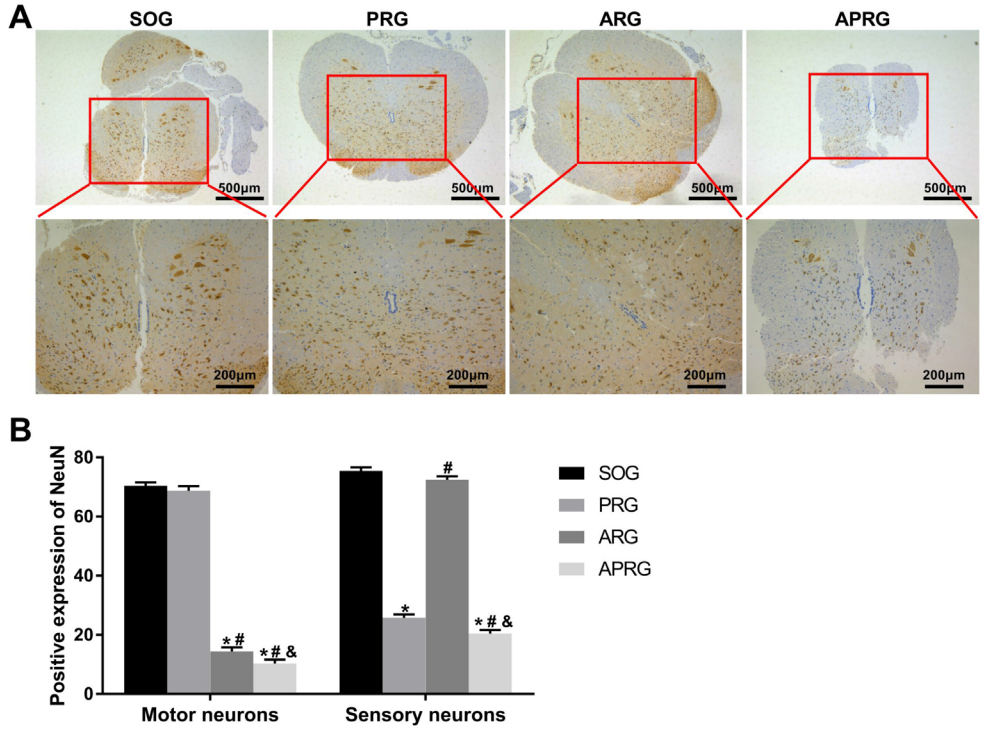

Figure 2. Positive expression of NeuN in spinal cord segments L_5 of selective sensory/motor nerve injury rats. Rats were subjected to posterior rhizotomy (PRG), anterior rhizotomy (ARG), or anterior combined with posterior rhizotomy (APRG). Sham-operated (SOG) rats served as control. (A-B) The expression of NeuN in motor neurons and sensory neurons of spinal cord segments L_5 was assessed by immunohistochemistry. There are two ways to distinguish sensory nerves or motor nerves in the spinal cord. First, the nerves in the posterior horn of normal spinal cord are sensory nerves, and the nerves in anterior horn are motor nerves. Second, the brown-yellow granules in sensory nerves are small and much, and the granules in motor nerves are and large and little. Scale bar=200 μm, 500 μm. *P<0.05 vs. SOG group; $^{\#}P$<0.05 vs. PRG group; $^{\&}P$<0.05 vs. ARG group.

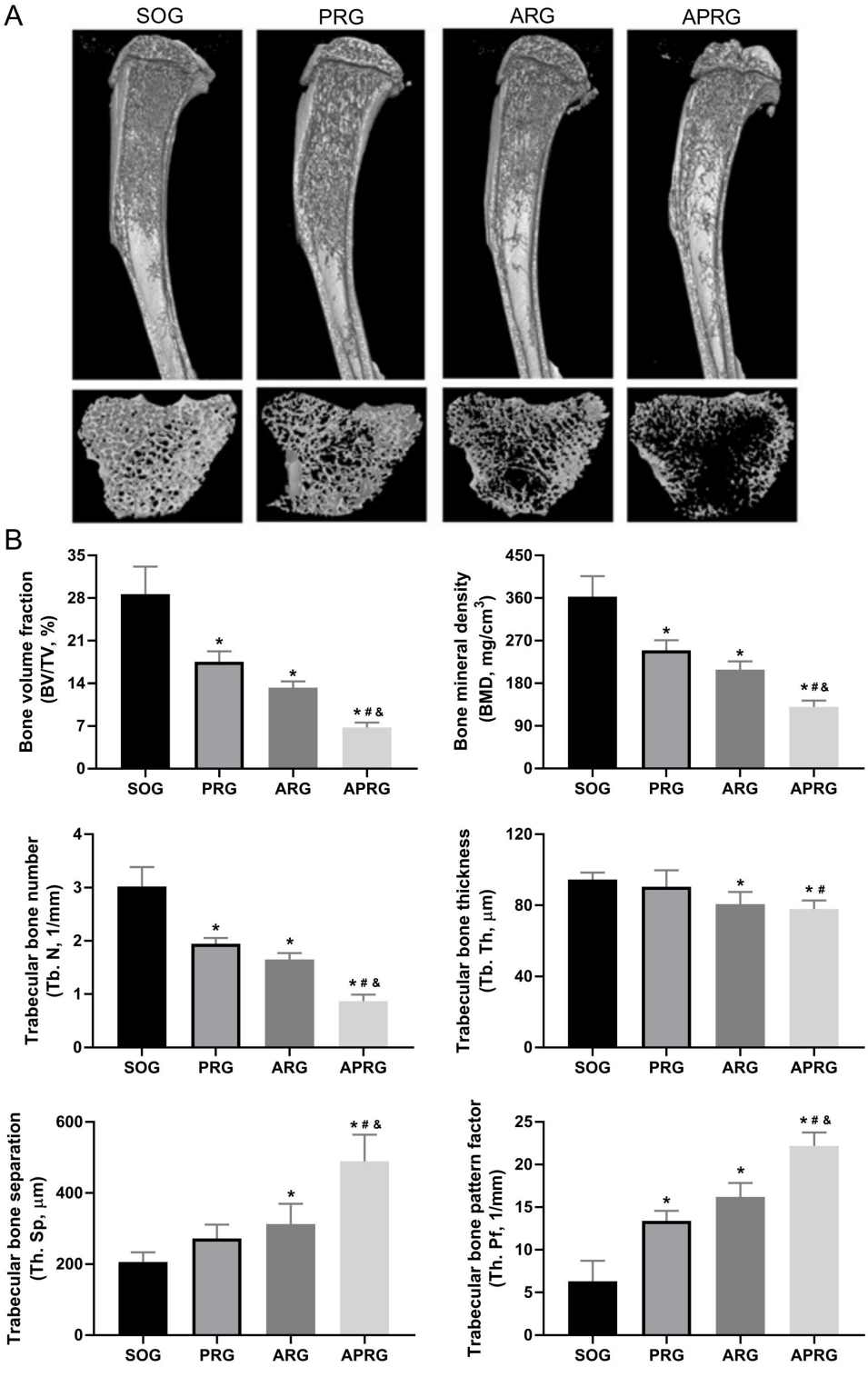

Figure 3. Three-dimensional reconstruction of tibial profile and cancellous bone of selective sensory/motor nerve injury rats. Rats were subjected to posterior rhizotomy (PRG), anterior rhizotomy (ARG), or anterior combined with posterior rhizotomy (APRG). Sham-operated (SOG) rats served as control. (A) The structural changes of the tibial profile and cancellous bone in rats were examined through micro-CT. (B) The bone quality parameters were analyzed.*P<0.05 vs. SOG group; $^{\#}P$<0.05 vs. PRG group; $^{\&}P$<0.05 vs. ARG group.

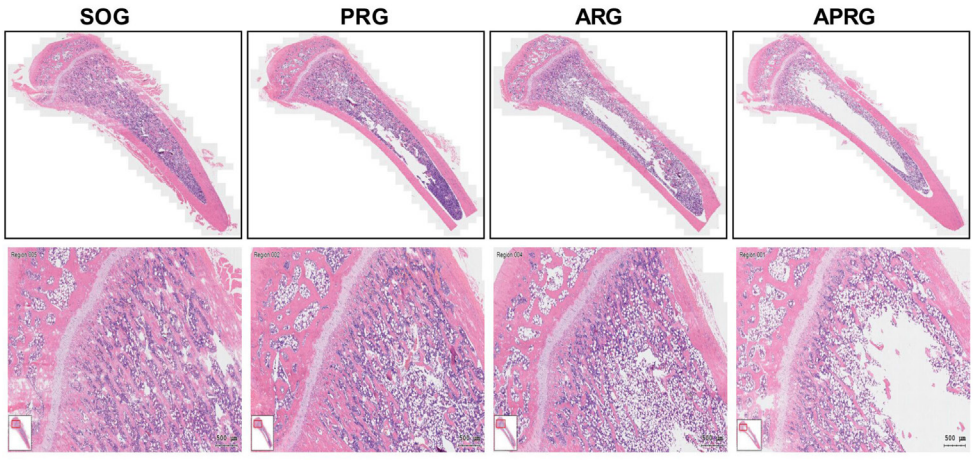

Figure 4. The pathological changes of trabecular bone in selective sensory/motor nerve injury rats. Rats were subjected to posterior rhizotomy (PRG), anterior rhizotomy (ARG), or anterior combined with posterior rhizotomy (APRG). Sham-operated (SOG) rats served as control. HE staining was performed to detect the pathological changes of trabecular bone in rats. Scale bar=500 μm.

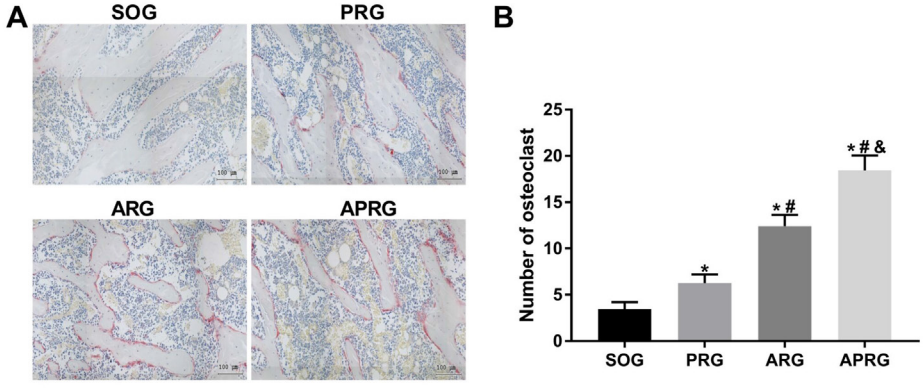

Figure 5. The number of osteoclasts in the tibial metaphysis of selective sensory/motor nerve injury rats. Rats were subjected to posterior rhizotomy (PRG), anterior rhizotomy (ARG), or anterior combined with posterior rhizotomy (APRG). Sham-operated (SOG) rats served as control. (A-B) TRAP staining was performed to assess the number of osteoclasts in the tibial metaphysis of rats. Scale bar=100 μm. *P<0.05 vs. SOG group; $^{\#}P$<0.05 vs. PRG group; $^{\&}P$<0.05 vs. ARG group.

selective sensory/motor nerve injury promoted the increase of osteoclasts and bone resorption in tibial tissues of rats.

Effects of selective sensory/motor nerve injury on the expression of relevant signalling pathway in rats

Finally, to determine the underlying mechanisms of sensory/motor nerve injury on bone metabolism, immunohistochemical staining and qRT-PCR were carried out to measure the expression of relevant signalling pathway in tibial tissues of rats. As shown in Figure 6A-B, CGRP, OCN and OPG expressions were severely decreased in PRG, ARG and ARPG groups, although at different extent. The expression of RANKL was markedly increased in PRG, ARG and ARPG groups, especially in ARPG group. Moreover, qRT-PCR results revealed that the expression of Wnt/β-catenin pathway-related genes, low-density lipoprotein receptor-related protein 5 (LRP5), RUNX2, Wnts1 and β-catenin, was significantly decreased in the ARG and APRG groups, but there was no significant change in the PRG group. The expression of PPARγ signalling pathway-related genes, PPARγ, lipoprotein lipase (LPL) and AP2, was increased in ARG and APRG groups, while the most significant increases was identified in the APRG group. Additionally, the expression

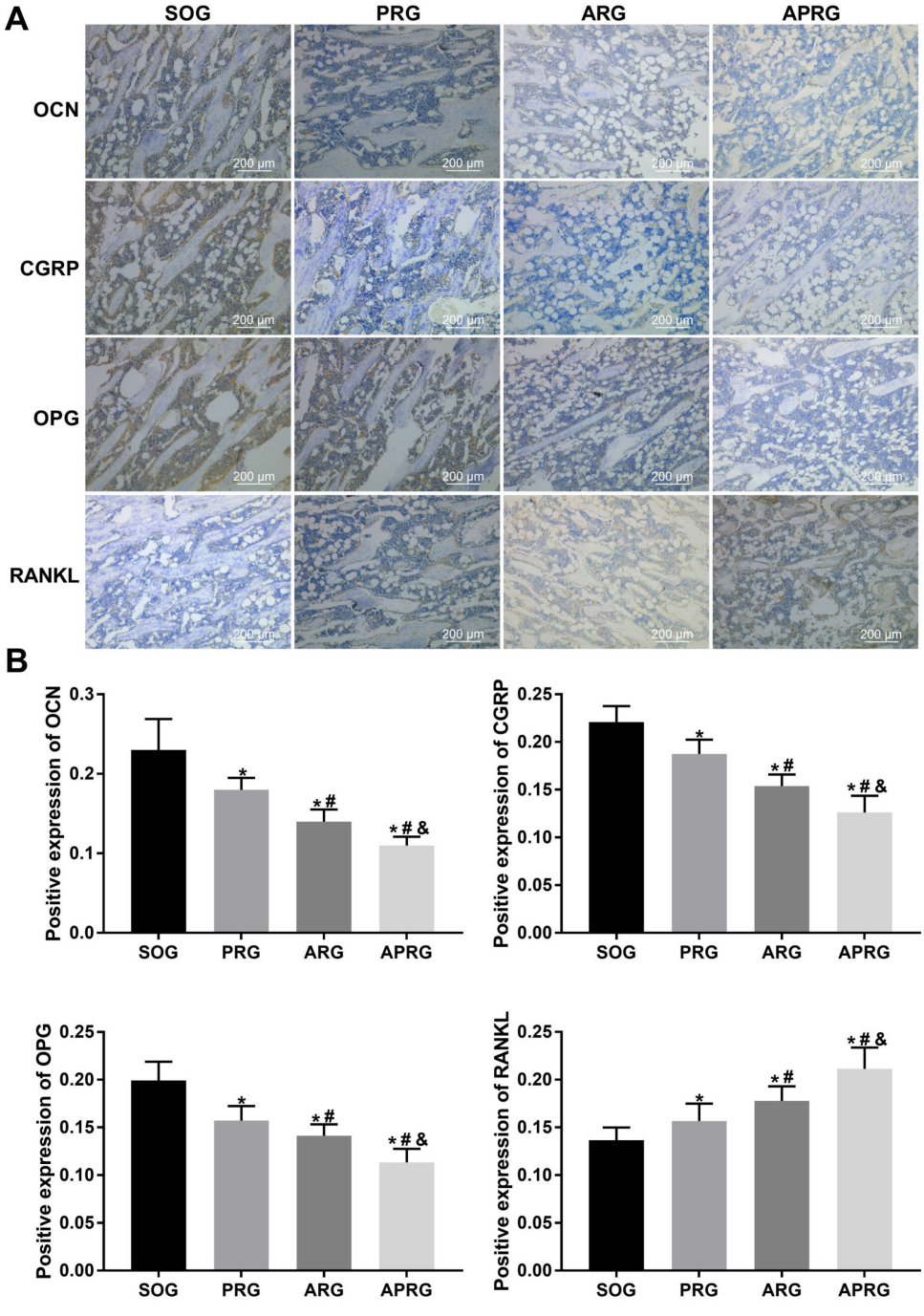

Figure 6. The expression of OCN, CGRP, OPG and RANKL in the tibial tissues of selective sensory/motor nerve injury rats. Rats were subjected to posterior rhizotomy (PRG), anterior rhizotomy (ARG), or anterior combined with posterior rhizotomy (APRG). Sham-operated (SOG) rats served as control. (A-B) Immunohistochemical staining was performed to examine the expression of OCN, CGRP, OPG and RANKL in the tibial tissues of rats. Scale bar=200 μm. *P<0.05 vs. SOG group; #P<0.05 vs. PRG group; &P<0.05 vs. ARG group.

of NF-κB signalling pathway-related genes, RANKL, NF-κB and tumor necrosis factor receptor-associated factor 6 (TRAF6), was significantly elevated in ARG and APRG group, while OPG expression was significantly decreased in PRG, ARG and APRG groups (Figure 7).

Discussion

Bones are tissues with metabolic function, and varying degrees of damage to the nervous system will affect bone metabolism and bone remodeling[18]. Previous studies have

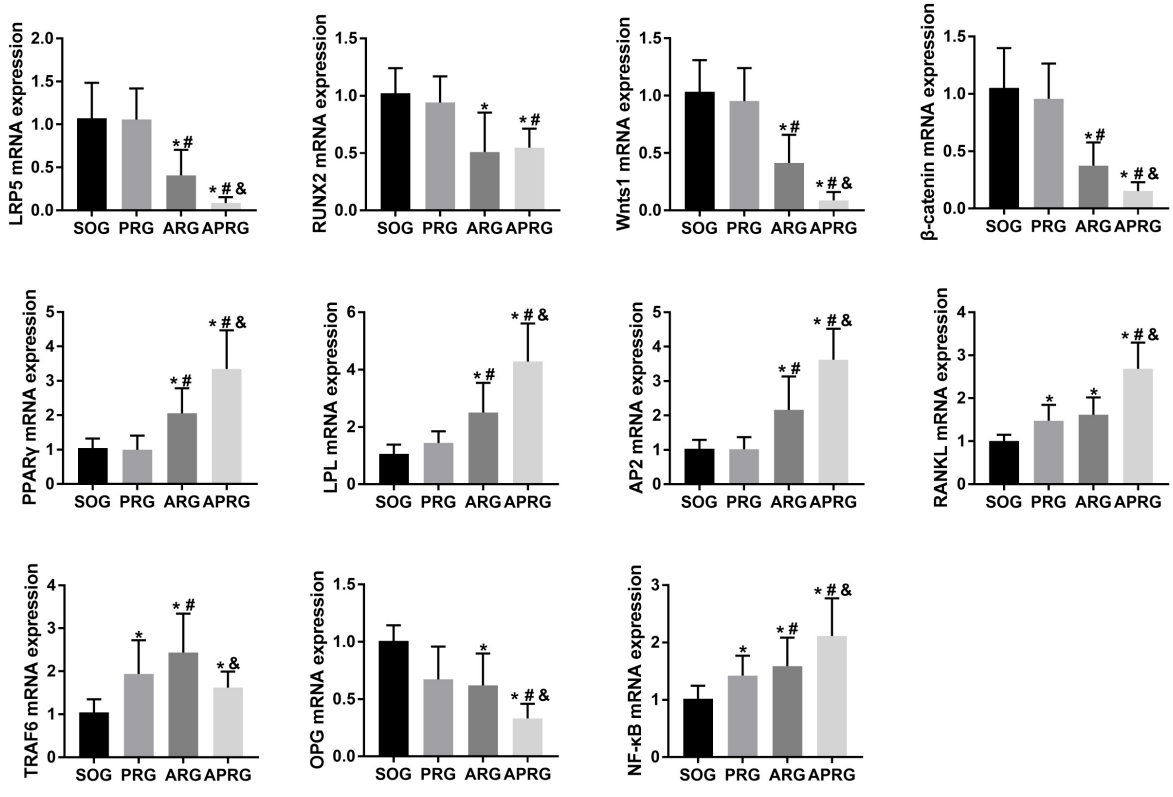

Figure 7. The expression of relevant signalling pathway-related genes in selective sensory/motor nerve injury rats. Rats were subjected to posterior rhizotomy (PRG), anterior rhizotomy (ARG), or anterior combined with posterior rhizotomy (APRG). Sham-operated (SOG) rats served as control. The qRT-PCR was performed to detect the expression of LRP5, RUNX2, Wnts1, β-catenin, PPARγ, LPL, AP2 RANKL, TRAF6, OPG and NF-κB in the tibial tissues of mice. **P*<0.05 vs. SOG group; #*P*<0.05 vs. PRG group; &*P*<0.05 vs. ARG group.

found that paraplegia patients exhibit osteoporosis in the lower limbs and bone loss in the upper limbs, which further verifies that nervous system is closely associated with osteoporosis after spinal cord injury[19,20]. In the present study, we established a selective sensory/motor nerve injury rat model through transecting $L_{4\text{-}6}$ sensory/motor nerve roots. The motor and sensory nerve transection had different effects on bone metabolism and bone remodeling. In the ARG group, the integrity of the trabecular bone was impaired, the number of trabecular bone was decreased, and the medullary cavity and bone separation were elevated. In PRG group, trabecular bone became thinner gradually, the number of trabecular bone was slightly decreased, bone fragility was increased and bone mineral density was decreased, but there was no obvious cavity in trabecular bone, and the integrity of trabecular bone was not damaged. Osteoporosis was obviously observed in the APRG group, and the plate-shaped trabecular bone became a rod-shaped structure. In some areas of APRG group, the thickness of trabecular bone became thinner, the width of the medullary cavity was increased, and the bone density was decreased. The bone loss in the APRG group was significantly more severe than that in the ARG and PRG groups. Collectively, the changes of bone remodeling and bone metabolism caused by the injury of different nerve components (sensory nerve or motor nerve) were different.

Wnt/β-catenin pathway plays a crucial role in bone metabolism[21]. A previous study has confirmed that Wnt/LRP5/β-catenin pathway regulates the activity and expression of Runx2, and thus affects bone metabolism and bone remodeling[22,23]. Under stimulations such as swimming and running, the expression of Wnt pathway effector protein β-catenin and the receptor protein LRP5 are increased, and the bone mineral density of mice is enhanced[24]. LRP5 knockdown inhibits the osteogenic capability of mice, and inhibition of Wnt pathway leads to ubiquitination of β-catenin[25], and thus causes the differentiation of BMSCs into adipocytes and ultimately promotes adipogenesis and suppresses osteogenesis[26,27]. Consistently, we found that inhibition of Wnt/β-catenin pathway caused a down-regulation of Wnts1, LRP5, Runx2, OPG and β-catenin in ARG and APRG groups. These two groups showed enhanced bone resorption and

reduced bone formation, which led to significantly stronger bone resorption than bone formation, that is, high turnover bone metabolism.

The NF-κB signalling pathway promotes osteoclast proliferation, differentiation, and maturation, and is located downstream of OPG/RANKL signalling pathway[28]. Changes of OPG/RANKL ratio are a key factor in maintaining the balance between bone metabolism and bone remodeling[29,30]. Appropriate mechanical forces can increase OPG expression and decrease RANKL expression in osteoblasts, thereby promoting bone formation and reducing bone resorption[31-33]. In the present work, we found that RANKL was increased in the PRG, ARG and APRG groups. TRAF6 was markedly up-regulated in the ARG group and slightly down-regulated in the PRG and ARPG groups. OPG expression was reduced in the PRG, ARG and APRG groups. Collectively, the changes of RANKL expression and the trend of OPG/RANKL ratio were consistent. In addition, NF-κB was increased in the PRG, ARG and APRG groups. These results suggest that the lack of mechanical force in rat bones promotes the activation and differentiation of osteoclasts and finally causes osteoporosis[34].

In this study, PPAR-γ, AP2, and LPL expressions were increased in the ARG and APRG groups, suggesting that PPAR-γ signalling pathway was activated. This pathway is mainly expressed in the immune system and adipose tissue and has a close relationship with body immunity, adipocyte differentiation, and glucose and lipid metabolism[35]. Another animal experiments have found that mice with heterozygous PPARγ gene reduces bone marrow fat and enhances bone mass[36], indicating that PPARγ is a critical factor in regulating differentiation of BMSCs[37]. When the PPARγ signalling pathway is activated and the Wnt/β-catenin pathway is inhibited, the promotion of BMP2 expression by BMSCs is inhibited, osteoblasts are decreased, and adipocytes are increased. They also inhibit the binding of Runx2 and OSE-2, thereby reducing osteocalcin[38], which is consistent with the conclusions of our experiments.

Both sensory and motor neurotomy can lead to the loss of bone mass and decrease in bone density, especially motor neurotomy. This is due to the activation or inhibition of the corresponding signalling pathways. In the ARG group, the PPAR-γ and NF-κB signalling pathways were activated, which led to enhanced bone resorption and decreased bone formation. The dynamic balance between osteogenesis and osteoclasts was biased towards the direction of osteoclasts.

Trabecular bone was characterized by high turnover of bone metabolism, and thus bone loss was more serious and faster. In the PRG group, the activated NF-κB pathway activating osteoclasts, and then reduced bone formation and increased bone resorption, thereby inhibiting the activity of osteoblasts. In addition, CGRP can directly act on osteoblasts to increase their activity. When sensory nerves are severed, CGRP secreted by neuropeptides is decreased, thereby leading to impaired osteoblast maturation. It is characterized by low-transformation bone metabolism, and thus the degree and speed of bone loss are lower than those of ARG and APRG group. In APRG group, the PPAR-γ and NF-κB pathways were activated, while the Wnt/β-catenin pathway was inhibited. The decrease of neuropeptide secretion reduces cAMP content, weakens the activity of Runx2 and inhibits bone formation. APRG group is characterized by high-transformation bone metabolism, and its bone loss is the most serious. In general, the bone loss in the PRG group was mainly due to decreased neuropeptides secreted by sensory nerves and activation of the NF-κB pathway, and less release of CGRP resulting in impaired osteoblast maturation. However, its effect on bone loss was limited and weaker than that in the ARG and APRG groups. Bone loss in the APG group was more severe than that in the PRG group. There were two main reasons, one was the lack of mechanical stress stimulation, which activated osteoclasts, and the balance between osteogenesis and osteoclast is broken. Ultimately, the osteoclast effect was greater than the osteogenesis effect. Second, the adipogenesis PPAR-γ signalling pathway was activated, and the adipogenesis was greater than the osteogenesis, resulting in obvious bone resorption and bone loss. The APRG group had the most severe bone loss, based on the superimposed effects of ARG and PRG groups. That is, the stimulation of neuropeptides and mechanical stress was also reduced, and PPAR-γ signalling in the adipogenic pathway was activated, which ultimately made the bone loss the most serious.

Conclusion

In summary, posterior rhizotomy and anterior rhizotomy induced the different degree of osteoporosis in rats. The former was mainly caused by inhibiting the Wnt signalling pathway to reduce neuropeptide substance. The latter was mainly caused by the activation of PPAR-γ signalling pathway and inhibition of Wnt pathway. This experiment has guiding significance for the clinical prevention and treatment of fracture, osteoporosis and other related diseases after nerve injury.

Ethical approval

Experimental procedures were approved by the Animal Ethics Committee of the Gannan Medical University.

Funding

This research was supported by Research Project of Jiangxi Provincial Department of Education(GJJ170888, GJJ170874), National Natural Science Foundation of China (81871355, 81974323), Natural Science Foundation of Guangdong Province (2019A1515011638, 2020A1515010055), Guangzhou Science and Technology Program Project (201804010082, 202002030485), Project of Jiangxi Health Committee (2018B002, 20195368, 20204484, 202210898) and Scientific Research Project of Gannan Medical University(ZD201705, YB201712).

References

1. Marrella A, Lee T, Lee D, Karuthedom S, Syla D, Chawla A, Khademhosseini A, Jang H. Engineering vascularized

and innervated bone biomaterials for improved skeletal tissue regeneration. Mater Today 2018;21(4):362-376.
2. Elefteriou F. Regulation of bone remodeling by the central and peripheral nervous system. Arch Biochem Biophys 2008;473(2):231-6.
3. Hofman M, Rabenschlag F, Andruszkow H, Andruszkow J, Möckel D, Lammers T, Kolejewska A, Kobbe P, Greven J, Teuben M, Poeze M, Hildebrand F. Effect of neurokinin-1-receptor blockage on fracture healing in rats. Sci Rep 2019;9(1):9744.
4. Hukkanen M, Konttinen Y, Santavirta S, Nordsletten L, Madsen J, Almaas R, Oestreicher A, Rootwelt T, Polak J. Effect of sciatic nerve section on neural ingrowth into the rat tibial fracture callus. Clin Orthop Relat Res 1995;(311):247-57.
5. Lips K, Kauschke V, Hartmann S, Thormann U, Ray S, Schumacher M, Gelinsky M, Heinemann S, Hanke T, Kautz A, Schnabelrauch M, Szalay G, Heiss C, Schnettler R, Alt V, Kilian O. Cholinergic nerve fibers in bone defects of a rat osteoporosis model and their regulation by implantation of bone substitution materials. J Musculoskelet Neuronal Interact 2014;14(2):173-88.
6. Nusse R, Clevers H. Wnt/β-Catenin Signaling, Disease, and Emerging Therapeutic Modalities. Cell 2017;169(6):985-999.
7. Chu Y, Gao Y, Yang Y, Liu Y, Guo N, Wang L, Huang W, Wu L, Sun D, Gu W. β-catenin mediates fluoride-induced aberrant osteoblasts activity and osteogenesis. Environ Pollut 2020;265:114734.
8. Zhou P, Li Y, Di R, Yang Y, Meng S, Song F, Ma L. H19 and Foxc2 synergistically promotes osteogenic differentiation of BMSCs via Wnt-β-catenin pathway. J Cell Physiol 2019;234(8):13799-13806.
9. Schupbach D, Comeau-Gauthier M, Harvey E, Merle G. Wnt modulation in bone healing. Bone 2020;138:115491.
10. Tian L, Yu X. Lipid metabolism disorders and bone dysfunction-interrelated and mutually regulated (review). Mol Med Rep 2015;12(1):783-94.
11. Go G. Low-Density Lipoprotein Receptor-Related Protein 6 (LRP6) Is a Novel Nutritional Therapeutic Target for Hyperlipidemia, Non-Alcoholic Fatty Liver Disease, and Atherosclerosis. Nutrients 2015;7(6):4453-64.
12. Vishal M, Vimalraj S, Ajeetha R, Gokulnath M, Keerthana R, He Z, Partridge N, Selvamurugan N. MicroRNA-590-5p Stabilizes Runx2 by Targeting Smad7 During Osteoblast Differentiation. J Cell Physiol 2017;232(2):371-380.
13. Kojetin D, Matta-Camacho E, Hughes T, Srinivasan S, Nwachukwu J, Cavett V, Nowak J, Chalmers M, Marciano D, Kamenecka T, Shulman A, Rance M, Griffin P, Bruning J, Nettles K. Structural mechanism for signal transduction in RXR nuclear receptor heterodimers. Nat Commun 2015;6:8013.
14. Wu M, Chen G, Li Y. TGF-β and BMP signaling in osteoblast, skeletal development, and bone formation, homeostasis and disease. Bone Res 2016;4:16009.
15. Yoo Y, Kwag J, Kim K, Kim C. Effects of neuropeptides and mechanical loading on bone cell resorption *in vitro*. Int J Mol Sci 2014;15(4):5874-83.
16. Scott-Solomon E, Boehm E, Kuruvilla R. The sympathetic nervous system in development and disease. Nat Rev Neurosci 2021;22(11):685-702.
17. Chen J, Zhang Y, Gao J, Li T, Gan X, Yu H. Sirtuin 3 deficiency exacerbates age-related periodontal disease. J Periodontal Res 2021;56(6):1163-1173.
18. Mabilleau G, Edmonds M. Role of neuropathy on fracture healing in Charcot neuro-osteoarthropathy. J Musculoskelet Neuronal Interact 2010;10(1):84-91.
19. Qin W, Bauman W, Cardozo C. Evolving concepts in neurogenic osteoporosis. Curr Osteoporos Rep 2010;8(4):212-8.
20. Qin W, Bauman W, Cardozo C. Bone and muscle loss after spinal cord injury: organ interactions. Ann N Y Acad Sci 2010;1211:66-84.
21. Ge X, Li Z, Zhou Z, Xia Y, Bian M, Yu J. Circular RNA SIPA1L1 promotes osteogenesis via regulating the miR-617/Smad3 axis in dental pulp stem cells. Stem Cell Res Ther 2020;11(1):364.
22. Long H, Zhu Y, Lin Z, Wan J, Cheng L, Zeng M, Tang Y, Zhao R. miR-381 modulates human bone mesenchymal stromal cells (BMSCs) osteogenesis via suppressing Wnt signaling pathway during atrophic nonunion development. Cell Death Dis 2019;10(7):470.
23. Yuan Z, Li Q, Luo S, Liu Z, Luo D, Zhang B, Zhang D, Rao P, Xiao J. PPARγ and Wnt Signaling in Adipogenic and Osteogenic Differentiation of Mesenchymal Stem Cells. Curr Stem Cell Res Ther 2016;11(3):216-25.
24. Yao C, Lv Y, Zhang C, Jin J, Xu L, Jiang J, Geng B, Li H, Xia Y, Wu M. MicroRNA-185 inhibits the growth and proliferation of osteoblasts in fracture healing by targeting PTH gene through down-regulating Wnt/β-catenin axis: In an animal experiment. Biochem Biophys Res Commun 2018;501(1):55-63.
25. Yao Q, Yu C, Zhang X, Zhang K, Guo J, Song L. Wnt/β-catenin signaling in osteoblasts regulates global energy metabolism. Bone 2017;97:175-183.
26. Ng L, Kaur P, Bunnag N, Suresh J, Sung I, Tan Q, Gruber J, Tolwinski N. WNT Signaling in Disease. Cells 2019;8(8):826.
27. Silva-García O, Valdez-Alarcón J, Baizabal-Aguirre V. Wnt/β-Catenin Signaling as a Molecular Target by Pathogenic Bacteria. Front Immunol 2019;10:2135.
28. Liu Y, Ai Y. Interleukin-20 Acts as a Promotor of Osteoclastogenesis and Orthodontic Tooth Movement. Stem Cells Int 2021;2021:5539962.
29. Chen X, Wang Z, Duan N, Zhu G, Schwarz E, Xie C. Osteoblast-osteoclast interactions. Connect Tissue Res 2018;59(2):99-107.
30. Zhang S, Wang X, Li G, Chong Y, Zhang J, Guo X, Li B, Bi Z. Osteoclast regulation of osteoblasts via RANK-RANKL reverse signal transduction *in vitro*. Mol Med Rep 2017;16(4):3994-4000.
31. Han Y, You X, Xing W, Zhang Z, Zou W. Paracrine and endocrine actions of bone-the functions of secretory proteins from osteoblasts, osteocytes, and osteoclasts.

Bone Res 2018;6:16.
32. Alzahrani M, Anam E, Makhdom A, Villemure I, Hamdy R. The effect of altering the mechanical loading environment on the expression of bone regenerating molecules in cases of distraction osteogenesis. Front Endocrinol 2014;5:214.
33. Zhang L, Liu W, Zhao J, Ma X, Shen L, Zhang Y, Jin F, Jin Y. Mechanical stress regulates osteogenic differentiation and RANKL/OPG ratio in periodontal ligament stem cells by the Wnt/β-catenin pathway. Biochim Biophys Acta 2016;1860(10):2211-9.
34. He Y, Liu S, Deng S, Kuang L, Xu S, Li Z, Xu L, Liu W, Ni G. Mechanical Stretch Promotes the Osteogenic Differentiation of Bone Mesenchymal Stem Cells Induced by Erythropoietin. Stem Cells Int 2019;2019:1839627.
35. Djouad F, Ipseiz N, Luz-Crawford P, Scholtysek C, Krönke G, Jorgensen C. PPARβ/δ: A master regulator of mesenchymal stem cell functions. Biochimie 2017; 136:55-58.
36. Cao Y, Balkan W, Hare J. S-nitrosylation and MSC-mediated body composition. Oncotarget 2015;6(30):28517-8.
37. Kim J, Lee Y, Kim J, Lee S, Bae M, Ahn J, Han D, Kwon B. PPARγ agonists induce adipocyte differentiation by modulating the expression of Lipin-1, which acts as a PPARγ phosphatase. Int J Biochem Cell Biol 2016;81:57-66.
38. Ahmadian M, Suh J, Hah N, Liddle C, Atkins A, Downes M, Evans R. PPARγ signaling and metabolism: the good, the bad and the future. Nat Med 2013;19(5):557-66.